
Modified gas-kinetic scheme for shock structures in argon

Wei Liao, Yan Peng and Li-Shi Luo*

Department of Mathematics and Statistics
and Center for Computational Sciences,
Old Dominion University,
Norfolk, Virginia 23529, USA
E-mail: wliao@odu.edu E-mail: ypeng@odu.edu
E-mail: lluo@odu.edu

*Corresponding author

Kun Xu

Department of Mathematics,
The Hong Kong University of Science and Technology,
Clear Water Bay, Kowloon, Hong Kong
E-mail: makxu@ust.hk

Abstract: The gas-kinetic scheme (GKS) is a finite-volume method in which the fluxes are constructed from the single particle velocity distribution function f . The distribution function f is obtained from the linearised Boltzmann equation and is retained only to the Navier-Stokes order in terms of the Chapman-Enskog expansion. Higher order non-equilibrium effects are included in a variable local particle collision time depending on local gradients of the hydrodynamic variables up to second order. The fluxes so constructed possess the non-equilibrium information beyond the linear constitutive relations and Fourier law. The modified gas-kinetic scheme with a local particle collision time λ^* depending on the gradients of hydrodynamic variables is used to compute shock structures in argon for Mach numbers between 1.2 and 25.0. We validate our results with existing numerical and experimental ones. Our results show that the modified gas-kinetic scheme is effective and efficient for shock structure calculations.

Keywords: collision time; gas kinetic scheme; GKS; non-equilibrium flow; shock structure in argon.

Reference to this paper should be made as follows: Liao, W., Peng, Y., Luo, L-S. and Xu, K. (2008) 'Modified gas-kinetic scheme for shock structures in argon', *Progress in Computational Fluid Dynamics*, Vol. 8, Nos. 1–4, pp.97–108.

Biographical notes: W. Liao is a Research Assistant Professor in the Department of Mathematics and Statistics, at Old Dominion University. He obtained his PhD Degree from National University of Singapore in 2004. Since 1999, his research focus has been in areas of aerodynamics and CFD methods and its applications.

Y. Peng is a Research Assistant Professor at the Department of Mathematics and Statistics at Old Dominion University. She obtained her PhD Degree from National University of Singapore in 2005. Since 1999, her research focus has been the lattice Boltzmann equation and its applications.

L-S. Luo is currently the Richard F. Barry Jr. Distinguished Endowed Professor at Department of Mathematics and Statistics, Old Dominion University. He obtained his PhD Degree in Physics from Georgia Institute of Technology in 1993. Before joining ODU in 2004, he worked in Los Alamos National Laboratory, Worcester Polytechnic Institute, ICASE/NASA Langley Research Center, and National Institute of Aerospace. His main research interests include kinetic theory, nonequilibrium flows, complex fluids, kinetic/mesoscopic methods for computational fluid dynamics, and scientific computing.

K. Xu is a Full Professor at the Department of Mathematics, Hong Kong University of Science and Technology (HKUST). He obtained his PhD Degree from the Astronomy Department, Columbia University in 1993. Before he joined HKUST in 1996, he was a Research Associate in the Department of Mechanical and Aerospace Engineering, Princeton University from 1993 to 1996. His research interesting has been focused on the development of gas-kinetic scheme and its application to multicomponent, MHD, and rarefied flows.

1 Introduction

Modelling and simulation of complex hypersonic flows with severe rarefaction effects and shock structures within the length scale of a few mean free paths present a challenging task for Computational Fluid Dynamics (CFD) (Holden, 2000). Such problems are genuinely multiscale in nature. The Knudsen number Kn , which is the ratio of the mean free path ℓ and a characteristic length scale L of the system, is a measure of the degree of rarefaction of the flow. Generally speaking, when both the Knudsen number and the Mach number are small, the flow is at or not far from thermodynamical equilibrium such that it can be adequately described by the continuum theory—the Navier-Stokes equations, which are the governing equations of classical hydrodynamics. However, within hypersonic shocks, the flow is far from thermodynamical equilibrium thus cannot be adequately described by the continuum theory. Hypersonic shock structures in gases have become a canonical test case for various numerical techniques for non-equilibrium flows (e.g., Torrilhon and Struchtrup, 2004; Struchtrup, 2005; Elizarova et al., 2005; Zheng et al., 2006).

In general, the Boltzmann equation is valid for non-equilibrium flows in the entire range of the Knudsen number and the Mach number. For non-equilibrium gas flows, the Direct Simulation Monte Carlo (DSMC) method (Bird, 1994) is the most commonly used solution method for the Boltzmann equation. The DSMC method is a stochastic method which is very effective for large-Knudsen-number flows, such as the free molecule flows with $Kn > 10$. However, the DSMC method has two severe limitations. First, the DSMC method is subject to fluctuations due to its stochastic nature, hence it requires averaging to obtain macroscopic flow fields. For time-dependent flows, DSMC simulations require ensemble averaging, which can be prohibitively expensive in terms of computational time. And second, the DSMC method becomes ineffective in near-continuum flow region of small Knudsen number, because its time step must be smaller than the mean free time, which can be extremely small in near-continuum flows. Because of these limitations, accurate DSMC simulations of realistic near-continuum flows are beyond the power of currently available computing resources. It is also difficult to couple the DSMC method with conventional CFD methods based on direct discretisations of the Navier-Stokes equations, which may be necessary in applications such as hypersonic vehicles and probes in Earth or Mars atmospheres.

To circumvent the limitations of the Navier-Stokes equation with the linear constitutive relations and the Fourier law, one is tempted to use higher-order equations such as the Burnett and super-Burnett equations (cf., Struchtrup, 2005 and references therein). Unfortunately, these higher-order equations are shown to be linearly unstable beyond certain some critical Mach number (cf., Struchtrup, 2005; Uribe et al., 2000), thus are difficult to be used for hypersonic shock structure calculations. On the other hand, numerically

solving the Boltzmann equation by using either the DSMC method or other means is computationally expensive for near-continuum hypersonic flows (Boyd and Gokcen, 1992; Bergemann and Brenner, 1994; Ivanov and Gimelshein, 1998; Wu and Tseng, 2003). Thus, there is a need for effective and efficient methods for near-continuum hypersonic flows (e.g., Schwartzentruber and Boyd, 2006; Schwartzentruber et al., 2007). In this work we intend to present a unified gas-kinetic method to compute shock structures in near-continuum hypersonic flows. The present method is based on the Gas-Kinetic Scheme (GKS) (Xu, 1998, 2001; Ohwada and Xu, 2004; Xu and Josyula, 2006), which is a finite-volume method derived from the Bhatnagar-Gross-Krook (BGK) equation (Bhatnagar et al., 1954). In the GKS method, the fluxes are constructed from the single particle distribution function f in phase space, which is the (approximated) solution of the Boltzmann equation. The fluxes so obtained possess the non-equilibrium information beyond the linear constitutive relations and the Fourier law, and therefore can capture non-equilibrium effects to certain extent. To accurately compute shock structures, higher-order effects are included in a variable local particle collision time depending on local gradients of the hydrodynamic variables up to second order.

The remaining part of this paper is organised as follows. In Section 2, we present the theoretical background of the gas-kinetic scheme for the compressible Navier-Stokes equations. We show in detail the construction of the GKS method based on the BGK equation (Bhatnagar et al., 1954). We then discuss the modification of the local collision time to capture shock structures and the correction of the unity Prandtl number intrinsic to the BGK model. In Section 3 we present our numerical results for shock structures in argon for Mach numbers between 1.2 and 25.0. We compute density, temperature, the stress and heat flux profiles across the shock, and compare our results with existing experimental data and numerical results obtained by the DSMC method and other means. Finally, we conclude this paper in Section 4.

2 Numerical methods

2.1 Gas Kinetic Scheme (GKS) for compressible flows

We shall describe the construction of the GKS for compressible flows (cf., Xu, 1998, 2001). We begin with the linearised Boltzmann equation (Struchtrup, 2005; Cercignani, 1988; Harris, 2004)

$$\partial_t f + \boldsymbol{\xi} \cdot \nabla f = \mathcal{L}(f, f), \quad (1)$$

where $f := f(\boldsymbol{x}, \boldsymbol{\xi}, \boldsymbol{\zeta}, t)$ is the single particle distribution function of space \boldsymbol{x} , particle velocity $\boldsymbol{\xi}$, particle internal degrees of freedom $\boldsymbol{\zeta}$ of dimension Z (including rotational, vibrational, electronic and other degrees of freedom), and time t ; \mathcal{L} is the linearised collision operator. For the sake of simplicity, and without losing generality in the context

of the linearised Boltzmann equation, we will use the Bhatnagar-Gross-Krook (Bhatnagar et al., 1954) (BGK) model for \mathcal{L} ,

$$\partial_t f + \boldsymbol{\xi} \cdot \nabla f = -\frac{1}{\lambda} [f - f^{(0)}]. \quad (2)$$

Here λ is the collision time and $f^{(0)}$ is the Maxwellian equilibrium distribution function in D dimensions (D is also the translational degrees of freedom of a particle),

$$f^{(0)} = \rho(\beta/2\pi)^{(D+Z)/2} e^{-\frac{1}{2}\beta(\mathbf{c} \cdot \mathbf{c} + \zeta \cdot \zeta)}, \quad (3)$$

where $\mathbf{c} := (\boldsymbol{\xi} - \mathbf{u})$ is the peculiar velocity, $\beta = (RT)^{-1}$, R is the gas constant, and ρ , \mathbf{u} and T are the density, flow velocity and temperature, respectively. The conserved variables are the conserved moments of the collision operator

$$\rho = \int f d\boldsymbol{\Xi} = \int f^{(0)} d\boldsymbol{\Xi}, \quad (4a)$$

$$\rho \mathbf{u} = \int f \boldsymbol{\xi} d\boldsymbol{\Xi} = \int f^{(0)} \boldsymbol{\xi} d\boldsymbol{\Xi}, \quad (4b)$$

$$\rho E = \frac{1}{2} \int f^{(0)} (\xi^2 + \zeta^2) d\boldsymbol{\Xi}, \quad (4c)$$

where E is the specific total energy and $\epsilon := \frac{1}{2}(D+Z)k_B T$ is the specific internal energy, k_B is the Boltzmann constant, and $\boldsymbol{\Xi} := (\boldsymbol{\xi}, \zeta)$ denotes the single particle velocity space and the internal degrees of freedom. The Maxwellian equilibrium leads to the equipartition of energy among the degrees of freedom, i.e., each degree of freedom shares the same amount of energy $k_B T/2$ at equilibrium.

By integrating along the characteristics, one can obtain the following solution of the BGK equation (2),

$$f(\mathbf{x} + \boldsymbol{\xi}t, t) = e^{-t/\lambda} f_0 + \frac{1}{\lambda} \int_0^t f^{(0)}(\mathbf{x}', t') e^{(t'-t)/\lambda} dt', \quad (5)$$

where $\mathbf{x}' := \mathbf{x} + \boldsymbol{\xi}t'$ and $f_0 := f(\mathbf{x}, \boldsymbol{\xi}, \zeta, t=0)$ is the initial state. The Gas-Kinetic Scheme (GKS) is formulated based on the above equation. With f_0 and $f^{(0)} := f^{(0)}(\mathbf{x}, \boldsymbol{\xi}, \zeta, t)$ given, one can construct an approximate solution for f at a later time $t > 0$.

The gas-kinetic scheme is a finite volume method for compressible flows. Thus, the values of the conserved variables are given at cell centres, while the values of fluxes are needed at cell boundaries. Unlike conventional CFD methods which evaluate fluxes from the hydrodynamic variables, the GKS computes the numerical fluxes from the distribution function f . We shall limit our discussion to two dimensions (2D), with the total number of internal degrees of freedom $Z = 1 + (5 - 3\gamma)/(\gamma - 1)$, accounting for the random motion in the z -direction and two rotational degrees of freedom, and $\gamma := c_p/c_v$ is the ratio of specific heats c_p and c_v .

For the sake of convenience, we shall use the following notation for the vectors of $(D+2)$ dimensions,

$$\boldsymbol{\Psi} := (1, \boldsymbol{\xi}, (\xi^2 + \zeta^2)/2)^\top, \quad (6a)$$

$$\mathbf{W} := (\rho, \rho \mathbf{u}, \rho E)^\top = \int f \boldsymbol{\Psi} d\boldsymbol{\Xi} = \int f^{(0)} \boldsymbol{\Psi} d\boldsymbol{\Xi}, \quad (6b)$$

$$\mathbf{F}_\alpha := \int f \boldsymbol{\Psi} \xi_\alpha d\boldsymbol{\Xi}, \alpha \in \{x, y\} := \{1, 2\}, \quad (6c)$$

$$\mathbf{h} := (\rho, \mathbf{u}, T)^\top, \quad (6d)$$

$$\mathbf{h}' := \left(\rho^{-1}, \beta \mathbf{u}, \frac{1}{2T} [\beta(c^2 + \zeta^2) - (D+Z)] \right)^\top, \quad (6e)$$

where \top denotes the transpose operator. In the above notation, $\boldsymbol{\Psi}$, \mathbf{W} , \mathbf{F}_α and \mathbf{h} have the collisional invariants, the conserved variables, the fluxes along the α -axis and the primitive variables as their components, respectively.

To simplify the ensuing discussion, we will only show the construction of the GKS in one dimension. Bear in mind that the GKS is a genuine multidimensional scheme. Since the advection operator in the Boltzmann equation is linear, operator splitting among D coordinates can be easily implemented. We denote a cell center at x coordinate by x_i , and its left and right cell boundaries by $x_{i-1/2}$ and $x_{i+1/2}$, respectively. For simplicity we set the initial time $t_0 = 0$, then the solution (5) at position x and time t is,

$$f(x, t) = e^{-t/\lambda} f_0(x - \xi_1 t) + \frac{1}{\lambda} \int_0^t f^{(0)}(x', t') e^{-(t-t')/\lambda} dt', \quad (7)$$

where $x' := x - \xi_1(t - t')$ is the x coordinate of the particle trajectory. In the above equation we omitted the variables in f which remain unchanged in time. Initially, only the values of the hydrodynamic variables, ρ , $\rho \mathbf{u}$ and ρE are given at the cell centre x_i , but the fluxes are to be evaluated at the cell boundaries $x_{i\pm 1/2}$. Therefore, both f_0 and $f^{(0)}(x', t')$ in the above equation are to be constructed from the hydrodynamic variables through the Boltzmann equation and Taylor expansion of $f^{(0)}$.

We can formally write the BGK equation (2) as

$$f = f^{(0)} - \lambda d_t f, \quad d_t := \partial_t + \boldsymbol{\xi} \cdot \nabla. \quad (8)$$

Thus, f can be solved iteratively, starting with $f = f^{(0)}$ on the right hand side of the above equation. For the purpose of simulating the Navier-Stokes equations, it is sufficient to use

$$f = f^{(0)} - \lambda d_t f^{(0)}.$$

The initial value can be approximated as

$$f_0 \approx [1 - \lambda(\partial_t + \xi_1 \partial_x)] f^{(0)} = [1 - \lambda \mathbf{h}' \cdot (\partial_t + \xi_1 \partial_x) \mathbf{h}] f^{(0)}. \quad (9)$$

In addition, the equilibrium $f^{(0)}$ can be expanded in a Taylor series about an arbitrary point $x = 0$,

$$f^{(0)}(x, t) \approx [1 + x \partial_x] f^{(0)}(0, t) = [1 + x \mathbf{h}' \cdot \partial_x \mathbf{h}] f^{(0)}(0, t). \quad (10)$$

By substituting Equations (10) into (9) we have

$$\begin{aligned} f_0(x, t) &\approx [1 + x\mathbf{h}' \cdot \partial_x \mathbf{h}] \\ &\quad \times [1 - \lambda \mathbf{h}' \cdot (\partial_t + \xi_1 \partial_x) \mathbf{h}] f^{(0)}(0, t) \\ &= 1 + ax - \lambda(a\xi_1 + A) f^{(0)}(0, t), \end{aligned} \quad (11)$$

where $a = \mathbf{h}' \cdot \partial_x \mathbf{h}$ and $A = \mathbf{h}' \cdot \partial_t \mathbf{h}$ are functions of ξ and the hydrodynamic variables, ρ , \mathbf{u} and T and their first order derivatives. They are related by the compatibility condition for f

$$\int f^{(n)} \Psi d\Xi = 0, \quad \forall n > 0,$$

where $f^{(n)}$ is the n -th order Chapman-Enskog expansion of f , and $f^{(0)}$ is the Maxwellian of Equation (10). Therefore, the first-order compatibility condition

$$\begin{aligned} \int f^{(1)} d\Xi &= -\lambda \int d_t f^{(0)} d\Xi \\ &= -\lambda \int (A + a\xi_1) f^{(0)} d\Xi = 0 \end{aligned}$$

leads to the relation between A and a ,

$$\int A f^{(0)} d\Xi = - \int a f^{(0)} \xi_1 d\Xi. \quad (12)$$

In computing the gradients $\partial_x \mathbf{h}$ for the coefficient a in Equation (11), we must assume that the hydrodynamic variables can be discontinuous at the cell boundary $x_{i+1/2}$ in general.

As for $f^{(0)}(x, t)$ in the integrand of Equation (7), it can be evaluated by its Taylor expansion,

$$\begin{aligned} f^{(0)}(x, t) &\approx (1 + t\partial_t + x\partial_x) f^{(0)}(0, 0) \\ &= f^{(0)}(0, 0) [1 + \mathbf{h}' \cdot (t\partial_t + x\partial_x) \mathbf{h}] \\ &= (1 + \bar{a}x + \bar{A}t) f^{(0)}(0, 0), \end{aligned} \quad (13)$$

where \bar{a} and \bar{A} are similar to a and A , respectively. The difference is that in \bar{a} the hydrodynamic variables are assumed to be continuous but not their gradients, while in a the hydrodynamic variables are assumed to be discontinuous. The details of how to evaluate a , A , \bar{a} and \bar{A} will be discussed next.

Assuming the hydrodynamic variables are discontinuous at the cell boundaries (or interfaces) of $x_{i+1/2} = 0$, then the values of the equilibrium $f^{(0)}$ on both sides of the cell boundary have to be evaluated differently. For the value $f_L^{(0)}$ on the left side, the hydrodynamic variables \mathbf{h} are interpolated to the left cell boundary $x_{i+1/2}^-$ with two points left and one point right of $x_{i+1/2}$, e.g., x_{i-1} , x_i and x_{i+1} . Then the left equilibrium value $f_L^{(0)}$ is computed from the hydrodynamic variables at $x_{i+1/2}^-$. Similarly, the right equilibrium value $f_R^{(0)}$ is evaluated from the hydrodynamic variables interpolated to $x_{i+1/2}^+$ with two points right and one point left of $x_{i+1/2}$, e.g., x_i , x_{i+1} and x_{i+2} . For Navier-Stokes flows, the van Leer

limiter is used in the interpolations (Xu, 2001; van Leer, 1974). However, no limiter is used when a shock is fully resolved, which will be discussed in the next section.

The gradients of the hydrodynamic variables are computed as the following:

$$\partial_x \mathbf{h}_L(x_{i+1/2}^-) = \frac{\mathbf{h}(x_{i+1/2}^-) - \mathbf{h}(x_i)}{x_{i+1/2}^- - x_i}.$$

Then the coefficient a_L at the left cell boundary $x_{i+1/2}^-$ is given by

$$a_L(x_{i+1/2}^-) = \mathbf{h}'_L(x_{i+1/2}^-) \cdot \partial_x \mathbf{h}_L(x_{i+1/2}^-).$$

As for the coefficient a_R at the right cell boundary $x_{i+1/2}^+$, the hydrodynamic variables are interpolated from the following three points: x_i , x_{i+1} , and x_{i+2} , and then

$$\begin{aligned} \partial_x \mathbf{h}_R(x_{i+1/2}^+) &= \frac{\mathbf{h}(x_{i+1/2}^+) - \mathbf{h}(x_{i+1})}{x_{i+1/2}^+ - x_{i+1}}, \\ a_R(x_{i+1/2}^+) &= \mathbf{h}'_R(x_{i+1/2}^+) \cdot \partial_x \mathbf{h}_R(x_{i+1/2}^+). \end{aligned}$$

With a_L and a_R given, A_L and A_R can be obtained immediately by using the compatibility condition (12).

The equilibria at the both sides of the cell boundary $x_{i+1/2}$ are $f_L^{(0)} := f^{(0)}(\xi, \mathbf{h}_L)$ and $f_R^{(0)} := f^{(0)}(\xi, \mathbf{h}_R)$, which are available now because \mathbf{h}_L and \mathbf{h}_R are given. In equilibrium $f^{(0)}$, the hydrodynamic variables are assumed to be continuous. Therefore, the conservative variables \mathbf{W} at the cell boundary $x_{i+1/2}$ are obtained by integrating the equilibrium at the both sides of the cell boundary,

$$\mathbf{W}(x_{i+1/2}) = \int_{\xi_x \geq 0} d\Xi \Psi f_L^{(0)} + \int_{\xi_x \leq 0} d\Xi \Psi f_R^{(0)}. \quad (14)$$

The above integrals for the density ρ and the energy ρE at the cell boundary lead to the error function

$$\text{erf}(z) = \frac{1}{\sqrt{\pi}} \int_0^z e^{-x^2} dx,$$

which can be easily computed. The hydrodynamic variables $\mathbf{h} := (\rho, \mathbf{u}, T)^\top$ can be easily obtained from the conservative variables $\mathbf{W} := (\rho, \rho \mathbf{u}, \rho E)^\top$, then the coefficients \bar{a}_L and \bar{a}_R are computed as the following,

$$\begin{aligned} \bar{a}_L(x_{i+1/2}^-) &= \mathbf{h}'(x_{i+1/2}^-) \cdot \frac{\mathbf{h}(x_{i+1/2}^-) - \mathbf{h}(x_i)}{x_{i+1/2}^- - x_i}, \\ \bar{a}_R(x_{i+1/2}^+) &= \mathbf{h}'(x_{i+1/2}^+) \cdot \frac{\mathbf{h}(x_{i+1/2}^+) - \mathbf{h}(x_{i+1})}{x_{i+1/2}^+ - x_{i+1}}. \end{aligned}$$

Note that in $\bar{a}_L(x_{i+1/2}^-)$ and $\bar{a}_R(x_{i+1/2}^+)$, both \mathbf{h} and \mathbf{h}' are continuous. Consequently, we have

$$\begin{aligned} f_0(x, t) &= [1 + a_R(x - \lambda\xi_1) - \lambda A_R] H(x) f_R^{(0)}(0, t) \\ &\quad + [1 + a_L(x - \lambda\xi_1) - \lambda A_L] H(-x) f_L^{(0)}(0, t), \end{aligned} \quad (15a)$$

$$\begin{aligned} f^{(0)}(x, t) &= [1 + H(-x)\bar{a}_L x \\ &\quad + H(x)\bar{a}_R x + \bar{A}t] f^{(0)}(0, 0), \end{aligned} \quad (15b)$$

where $H(x)$ is the Heaviside function. Finally, the value of f at a cell boundary can be obtained by substituting the above equations of $f_0(x, t)$ and $f^{(0)}(x, t)$ into Equation (7),

$$\begin{aligned} f(x_{i+1/2}, t) = & \{ [(1 - \bar{A}\lambda)(1 - e^{-t/\lambda}) + \bar{A}t] \\ & + [(t + \lambda)e^{-t/\lambda} - \lambda] [\bar{a}_L H(\xi_1) + \bar{a}_R H(-\xi_1)] \xi_1 \} f_0^{(0)} \\ & + e^{-t/\lambda} \{ [(1 - \xi_1(t + \lambda)a_L) - \lambda A_L] H(\xi_1) f_{0L}^{(0)} \\ & + [(1 - \xi_1(t + \lambda)a_R) - \lambda A_R] H(-\xi_1) f_{0R}^{(0)} \}, \end{aligned} \quad (16)$$

where $f_0^{(0)}$, $f_{0L}^{(0)}$ and $f_{0R}^{(0)}$ are initial values of $f^{(0)}$, $f_L^{(0)}$ and $f_R^{(0)}$ evaluated at the cell boundary $x_{i+1/2}$. The only unknown in $f(x_{i+1/2}, t)$ of Equation (16) is the coefficient \bar{A} . By using $f^{(0)}(x_{i+1/2}, t)$ of Equation (15b) and $f(x_{i+1/2}, t)$ of Equation (16), the conservation laws lead to the following equation,

$$\begin{aligned} & \int_0^{\Delta t} dt \int d\Xi \Psi f^{(0)}(x_{i+1/2}, t) \\ & = \int_0^{\Delta t} dt \int d\Xi \Psi f(x_{i+1/2}, t), \end{aligned}$$

which is used to determine \bar{A} in terms of a_L , a_R , \bar{a}_L , and \bar{a}_R . Therefore, $f^{(0)}(x_{i+1/2}, t)$ is fully determined from the hydrodynamic variables at the cell centers about the cell boundary $x_{i+1/2}$.

The relaxation time λ in Equation (16) has yet to be determined. In the gas-kinetic scheme for compressible flows, the particle collision time is determined by the local macroscopic flow variables through

$$\lambda = \frac{\mu}{p} = \frac{\mu\beta}{\rho}, \quad (17)$$

where μ is the dynamic viscosity and p is the pressure. The above relation between λ , μ and p is valid when the flow fields are continuous. When discontinuity is considered as for compressible flows with shocks, one must introduce some artificial dissipation to capture shocks (Xu, 2001). In the GKS method, the artificial dissipation is introduced by modifying the relaxation time λ as the following:

$$\lambda = \frac{\mu(x_{i+1/2})}{p(x_{i+1/2})} + \sigma \Delta t \frac{(p_L - p_R)}{(p_L + p_R)} = \lambda_0 + \sigma \lambda_1, \quad (18)$$

where λ_0 and $\sigma \lambda_1$ represent the physical and artificial mean free times, respectively. The value of the dynamic viscosity $\mu(x_{i+1/2})$ is determined by Sutherland's formula:

$$\mu = \mu_0 \frac{(T_0 + C)}{(T + C)} \left(\frac{T}{T_0} \right)^{3/2} = \mu_0 \frac{(1 + CR\beta_0)}{(1 + CR\beta)} \left(\frac{\beta_0}{\beta} \right)^{1/2}, \quad (19)$$

where μ_0 , T_0 and C are material-dependent constants, and $\beta := 1/RT$ and $\beta_0 := 1/RT_0$. Specifically, we use $\lambda_0 = \mu/p = \mu\beta/\rho$, in which the value of $\lambda_0(x_{i+1/2})$ is computed from the values of $T(x_{i+1/2})$ and $\rho(x_{i+1/2})$ at

the previous time step $t = t_{n-1}$, given by the hydrodynamic variables $\mathbf{h}(x_{i+1/2})$ through $\mathbf{W}(x_{i+1/2})$ of Equation (14).

It should be noted that the relaxation time λ is not a constant, according to Equation (17). In kinetic theory (Struchtrup, 2005; Cercignani, 1988; Harris, 2004), both the viscosity μ and the heat conductivity κ are independent of the density ρ but they are functions of temperature T . Consequently, we must have $\lambda \propto 1/\rho$. By using Sutherland's formula (19), this criterion is satisfied.

The term of $\sigma \lambda_1$ in Equation (18) gives rise to an artificial dissipation, which can be tuned by the parameter $\sigma \in [0, 1]$. The values of pressure p evaluated at the left and the right of the cell boundary $x_{i+1/2}$, $p_L = p(x_{i+1/2}^-)$ and $p_R = p(x_{i+1/2}^+)$, are obtained from $\mathbf{h}(x_{i+1/2}^-)$ and $\mathbf{h}(x_{i+1/2}^+)$, respectively. Therefore, the artificial dissipation is in effect only when shocks are treated as discontinuities. Obviously, when flow fields are continuous, $p_L = p_R$, and the artificial dissipation vanishes.

With f given at the cell boundaries, the time-dependent fluxes can be evaluated,

$$\mathbf{F}_\alpha^{i+1/2,j} = \int \xi_\alpha \Psi f(x_{i+1/2}, t) d\Xi. \quad (20)$$

By integrating the above equation over each time step, we obtain the total fluxes as

$$\bar{\mathbf{F}}_x^{i\pm 1/2,j} = \int_0^{\Delta t} \mathbf{F}_x^{i\pm 1/2,j} dt, \quad (21a)$$

$$\bar{\mathbf{F}}_y^{i,j\pm 1/2} = \int_0^{\Delta t} \mathbf{F}_y^{i,j\pm 1/2} dt. \quad (21b)$$

Then the flow governing equations in the finite volume formulation can be written as

$$\begin{aligned} \mathbf{W}_{ij}^{n+1} = & \mathbf{W}_{ij}^n - \frac{1}{\Delta x} (\bar{\mathbf{F}}_x^{i+1/2,j} - \bar{\mathbf{F}}_x^{i-1/2,j}) \\ & - \frac{1}{\Delta y} (\bar{\mathbf{F}}_y^{i,j+1/2} - \bar{\mathbf{F}}_y^{i,j-1/2}), \end{aligned} \quad (22)$$

which are used to update the flow field.

2.2 Modified Gas Kinetic Scheme (GKS) for near-continuum flows

In the near-continuum or transition flow regime, the mean free time λ is no longer a function of hydrodynamic variables alone as given by Equation (17). In other words, the simple constitutive relations in the framework of continuum theory are no longer valid in the non-equilibrium flows. This is clear from the derivation of the BGK equation (e.g., Struchtrup, 2005; Cercignani, 1988; Harris, 2004),

$$\begin{aligned} & \int d\xi_2 d\theta d\epsilon B(\theta, \|\xi_1 - \xi_2\|) f_1' f_2' \\ & \approx f_1^{(0)} \int d\xi_2 d\theta d\epsilon B(\theta, \|\xi_1 - \xi_2\|) f_2^{(0)} \\ & = \frac{1}{\lambda(\xi_1)} f_1^{(0)}, \end{aligned} \quad (23)$$

where the post-collision distribution function f'_i is approximated by the equilibrium $f_i^{(0)}$, and the relaxation time λ is a function of ξ_1 unless $B(\theta, \|\xi_1 - \xi_2\|)$ is independent of $\|\xi_1 - \xi_2\|$, which is true only for the Maxwell molecules (Struchtrup, 2005; Cercignani, 1988; Harris, 2004; Chapman and Cowling, 1952). It is clear that in general the mean free time λ depends on the molecular velocity ξ_1 and the inter-molecular interaction included in $B(\theta, \|\xi_1 - \xi_2\|)$. Therefore, to accurately compute shock structures, within which the flow deviates from the equilibrium and the Navier-Stokes equations are no longer valid, one would need to solve the Boltzmann equation, by using DSMC method or other means. On the other hand, one can also attempt to extend the validity of the Navier-Stokes equations through the regularisation of the Chapman-Enskog expansion (Rosenau, 1989). The modified GKS method for non-equilibrium flows used in this work is indeed such an approach (Xu and Josyula, 2006; Xu and Tang, 2004).

The basic idea behind the modified GKS for shock structures is the following. We know that the conservation laws are valid everywhere, even within shocks and at microscopic level. What breaks down within shocks are the linear constitutive relations and the Fourier law. The extend of shock structures is of the order of a few mean free paths. Within a shock, it is no longer adequate to assume that the mean free time $\lambda = \mu/p$, which is a hydrodynamic description, because λ would depend not only on the hydrodynamic variables, but also on their gradients, as well as the microscopic inter-molecular potential, as indicated by Equation (23). Consequently, from the standpoint of generalised hydrodynamics, the transport coefficients depend on both the hydrodynamic variables and their gradients. For the modified GKS method, a self-consistent iterative solution of the BGK equation is used to approximate the generalised transport coefficients. In what follows we shall consider a one-dimensional case for the sake of simplicity.

We will use the BGK equation to illustrate our idea,

$$f = f^{(0)} - \lambda d_t f = f^{(0)} - \lambda(\partial_t + \xi_1 \partial_x) f. \quad (24)$$

Suppose we can modify the relaxation time such that it depends on flow fields and their gradients, and the form of the Navier-Stokes equations remains intact, i.e.,

$$f \approx f^{(0)} - \lambda^* d_t f^{(0)} := f^{[1]}, \quad (25)$$

where λ^* is the modified relaxation time. On the other hand, we can iterate Equation (24) once more,

$$f \approx f^{(0)} - \lambda d_t f^{(1)} = f^{(0)} - \lambda d_t f^{(0)} + \lambda \lambda^* d_t^2 f^{(0)} := f^{[2]}, \quad (26)$$

and assume that the modelling of λ^* is sufficiently accurate to take into account the effects due to higher order derivatives of the hydrodynamic variables. Therefore, we have $f^{[1]} \approx f^{[2]}$, which leads to

$$\lambda^* d_t f^{(0)} \approx \lambda(d_t f^{(0)} - \lambda^* d_t^2 f^{(0)}). \quad (27)$$

To compute the value of λ^* , the above equation must be averaged over some function ϕ of ξ so that

$$\lambda^* (\langle d_t f^{(0)} \rangle + \lambda \langle d_t^2 f^{(0)} \rangle) \approx \lambda \langle d_t f^{(0)} \rangle,$$

then we can obtain the modified relaxation time

$$\lambda^* = \frac{\lambda}{1 + \lambda \langle d_t^2 f^{(0)} \rangle / \langle d_t f^{(0)} \rangle}, \quad (28a)$$

$$\langle d_t f^{(0)} \rangle := \int d_t f^{(0)} \phi(\xi) f d\Xi, \quad (28b)$$

$$\langle d_t^2 f^{(0)} \rangle := \int d_t^2 f^{(0)} \phi(\xi) f d\Xi. \quad (28c)$$

Because the stress and the heat conduction terms are different moments of the distribution function f , the values of λ^* for these terms should also be treated differently. We use $\phi(\xi) = c^2$ for the relaxation time corresponding to the viscosity coefficient and $\phi(\xi) = c_\alpha(c^2 + \zeta^2)$ for relaxation time corresponding to the heat conductivity coefficient in α -direction. In effect, $\langle d_t^2 f^{(0)} \rangle$ and $\langle d_t f^{(0)} \rangle$ are computed as the functions of hydrodynamic variables as well as their spatial and temporal derivatives up to second order.

To maintain numerical stability, the following *empirical* nonlinear dynamic limiter is imposed on λ^* ,

$$\lambda^* = \frac{\lambda}{1 + \max \left[B_1, \lambda \min \left(B_2, \frac{\langle d_t^2 f^{(0)} \rangle}{\langle d_t f^{(0)} \rangle} \right) \right]}, \quad (29)$$

to guarantee that $\lambda^* \geq \lambda$ and to minimise the large numerical fluctuation caused by vanishingly small $\langle d_t f^{(0)} \rangle$, which can occur in regions outside the shock, through two parameters $B_1 < 0$ and $B_2 \leq 0$, which set lower and upper bounds of the denominator in the limiter, respectively. The idea behind the limiter of Equation (29) is rather simple and it includes two considerations. The first consideration is based on the observation that the shock thickness obtained by a Navier-Stokes solver is usually thinner than it should be with a given viscosity depending on temperature T (Alsmeyer, 1976), and that the stress within the shock layer is larger than the value predicted by the Navier-Stokes equations (Elliot, 1975). Therefore, we require that $\lambda^* > \lambda > 0$ within shock. We observe that usually $\langle d_t^2 f^{(0)} \rangle / \langle d_t f^{(0)} \rangle < 0$. Therefore $\lambda^* > \lambda$ if $0 > \lambda \langle d_t^2 f^{(0)} \rangle / \langle d_t f^{(0)} \rangle > -1$. And the second consideration is numerical stability. The numerator in Equation (28a) may be too close to zero or even become negative in the presence of numerical noise, which is unphysical. Also, outside the shock layer, both $d_t f^{(0)}$ and $d_t^2 f^{(0)}$ may be vanishingly small. Therefore, a lower bound for the numerator is required, which is set by $B_1 = -0.5$ here. We set the parameter $B_2 = -0.1$ unless otherwise stated. The limiter of Equation (29) satisfies both criteria. The values of the lower and upper bounds are chosen empirically. As we will show later, this empirical limiter works well indeed.

Obviously the λ^* is a continuous function of the local hydrodynamic variables and their derivatives. It does not have the part in Equation (18) corresponding to an artificial

dissipation, because the flow fields are assumed to be continuous and well resolved within a shock in this case. Therefore, it should be emphasised that no limiter is used in the interpolations of hydrodynamic variables when a shock is fully resolved.

2.3 Prandtl number correction

The relaxation time λ in the BGK model determines both the dynamic viscosity μ and the heat conductivity κ , which results in the unit Prandtl number $\text{Pr} = \mu/\kappa = 1$. However, this defect can be easily removed by simply replacing the coefficient λ in the heat flux \mathbf{q} by the appropriate one determined by the Prandtl number Pr in the total energy flux \mathbf{K} (Xu, 2001; Woods, 1993),

$$\mathbf{K}^{\text{new}} = \mathbf{K} + \left(\frac{1}{\text{Pr}} - 1\right)\mathbf{q}, \quad (30a)$$

$$\mathbf{K} := \frac{1}{2} \int (\xi^2 + \zeta^2) \xi f d\Xi, \quad (30b)$$

where \mathbf{q} is the time-dependent heat flux,

$$\mathbf{q} := \frac{1}{2} \int (c^2 + \zeta^2) c f d\Xi. \quad (31)$$

Since the distribution function f is assumed to be smooth, it can be approximated by Xu (2001)

$$f = f_0^{(0)} [1 - \lambda(\bar{a}\xi_1 + \bar{A}) + t\bar{A}]. \quad (32)$$

Consequently the heat flux \mathbf{q} can be approximated by

$$\begin{aligned} q_\alpha &\approx -\lambda \int f_0^{(0)} (\bar{a}\xi_\alpha + \bar{A}) (\psi_4 - \mathbf{u}_0 \cdot \xi) \xi_\alpha d\Xi \\ &:= \lambda q'_\alpha, \end{aligned} \quad (33a)$$

$$\psi_4 := \frac{1}{2} (\xi^2 + \zeta^2), \quad \alpha \in \{x, y\} := \{1, 2\}, \quad (33b)$$

where $\mathbf{u}_0 := (u_0, v_0)$ is the flow velocity at the cell interface and at time $t = 0$. In the above evaluation of q_α , the term $t\bar{A}$ in Equation (32) has been neglected. This approximation would only affect the temporal accuracy of the GKS. Since all moments needed in Equation (33) have been computed in the evaluation of the total energy flux \mathbf{K} , additional effort required to compute \mathbf{K}^{new} is negligible. Finally, Equation (30a) can be written as

$$\mathbf{K}^{\text{new}} = \mathbf{K} + \left(\frac{1}{\text{Pr}} - 1\right)\lambda\mathbf{q}'. \quad (34)$$

For the near-continuum flows, the modified variable relaxation time λ^* given by Equation (29) must be used in computing the energy flux. Because different relaxation times must be used for the viscous stress and the heat flux, as indicated in the discussion following Equations (28) and (34) is modified as

$$\mathbf{K}^{\text{new}} = \mathbf{K} + \left(\frac{\lambda_\kappa^*}{\text{Pr}} - \lambda_\mu^*\right)\mathbf{q}', \quad (35)$$

where λ_κ^* and λ_μ^* are the modified relaxation times corresponding to the heat conductivity κ and the viscosity μ , respectively, and they are computed according to Equations (28).

3 Shock structures in argon

We use the modified GKS with a variable local collision time to compute shock structures in argon with Mach number between 1.2 and 25.0. We calculate the density, temperature, stress, and heat flux profiles across one-dimensional stationary shock waves in argon and compare our results with a direct solution of the Boltzmann equation (Ohwada, 1993), DSMC results (Bird, 1970), and available experimental measurements (Alsmeyer, 1976; Reese et al., 1995; Schmidt, 1969).

The computational domain is covered with a uniform mesh with at least 30 points within the shock. Although the stationary shock wave is one-dimensional, we use a two-dimensional code in which there are only three grid points with periodic boundary conditions in y direction. The entire computation domain in x direction is so extended that the shock disturbance has no effect in either upstream and downstream boundaries. For a one-dimensional stationary shock wave, the initial conditions are the upstream Mach number, temperature T_1 and pressure p_1 ; the downstream conditions T_2 and p_2 are obtained via the Rankine-Hugoniot conditions. Other parameters for argon are: $\gamma = 5/3$, $\text{Pr} = 2/3$ and $\mu \propto T^s$, with $s = 1/2 + 2/(\nu - 1)$, where ν is the exponent of the inverse power law for inter-molecular force (Bird, 1994). The upstream mean free path λ_1 is defined by Bird (1994),

$$\lambda_1^{(1)} = \frac{2\mu(7 - 2s)(5 - 2s)}{15\rho_1\sqrt{2\pi RT_1}}. \quad (36)$$

or (Alsmeyer, 1976)

$$\lambda_1^{(2)} = \frac{16\mu}{5\rho_1\sqrt{2\pi RT_1}}. \quad (37)$$

Both definitions of λ_1 are used so that the comparisons with existing data (Bird, 1994; Alsmeyer, 1976) are possible. The quantities of interest are the density and temperature distributions,

$$\frac{\delta\rho}{\Delta\rho} := \frac{(\rho - \rho_1)}{(\rho_2 - \rho_1)}, \quad \frac{\delta T}{\Delta T} := \frac{(T - T_1)}{(T_2 - T_1)},$$

where ρ_2 and T_2 are the downstream density and temperature, respectively, and the heat flux q_x and the stress τ_{xx} ,

$$q_x := \kappa\partial_x T, \quad \tau_{xx} := \frac{4}{3}\mu\partial_x u,$$

where the derivatives $\partial_x T$ and $\partial_x u$ are computed by using second-order central difference, and the transport coefficients are given by:

$$\kappa = \frac{\gamma R}{(\gamma - 1)\text{Pr}}\mu, \quad \mu = \lambda_\mu^* p = \lambda_\mu^* \frac{\rho}{\beta}.$$

Thus one still assumes the form of linear constitutive relations for both the heat flux q_x and the stress τ_{xx} , however, the viscosity μ and the heat conductivity κ depend on the gradients of the hydrodynamic variables as well, as in generalised hydrodynamics. The linear constitutive relations are also used to measure the heat flux q_x and the stress τ_{xx} in DSMC simulations (e.g., Bird, 1970).

Figure 1 Mach-1.2 shock structures in argon. The density and temperature profile (left), the normalised heat flux $q_x/p_1(2RT_1)^{3/2}$ (centre), and the normalised stress τ_{xx}/ρ_1RT_1 (right). The lines are the modified-GSK results and symbols are the solutions of the Boltzmann equation (Ohwada, 1993)

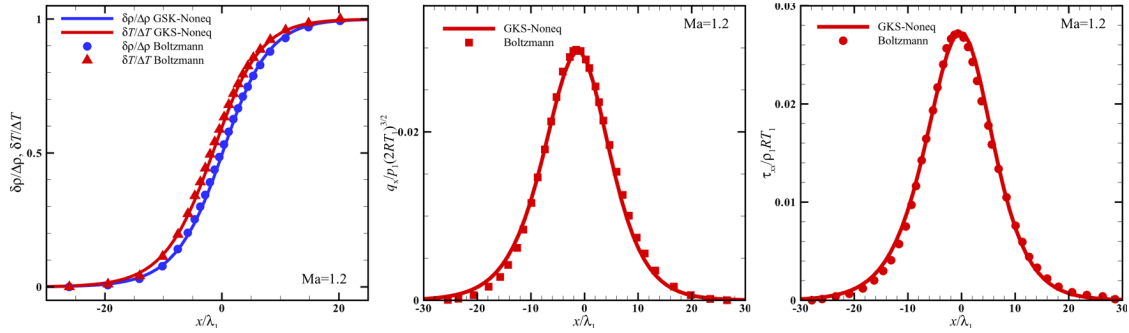


Figure 2 Mach-2 shock structures in argon. Same as Figure 1

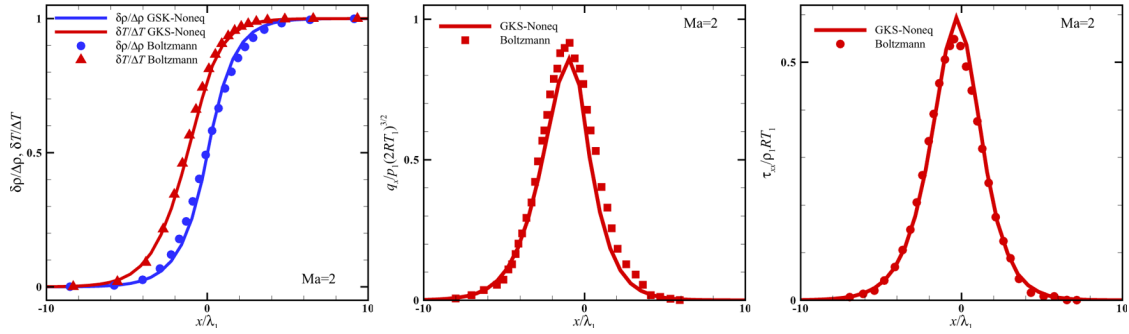
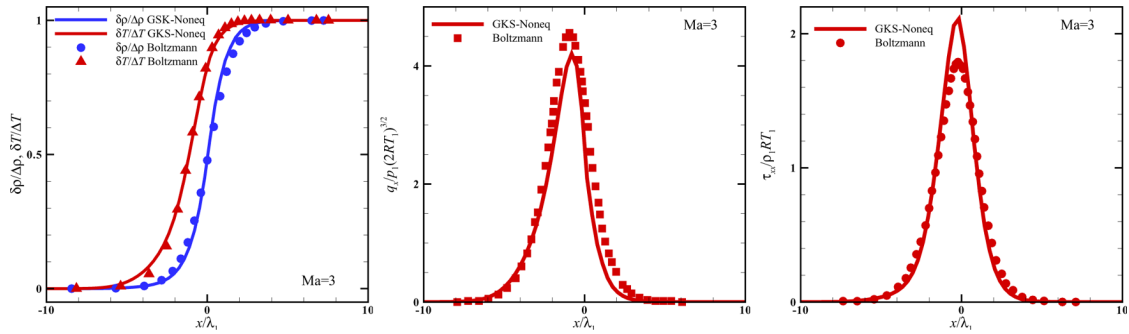


Figure 3 Mach-3 shock structures in argon. Same as Figure 1

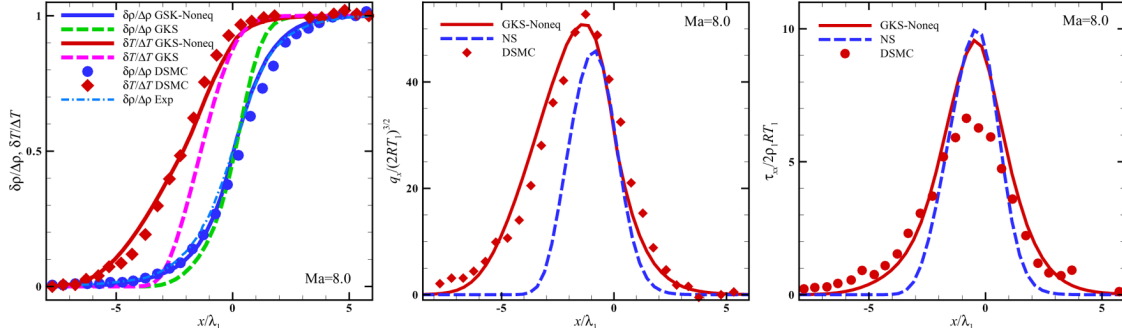


We first compute the stationary shock structure in argon at low Mach numbers at 1.2, 2.0 and 3.0. Argon molecules are modelled as hard spheres with $\nu = \infty$, e.g., $s = 0.5$. Figures 1–3 show the profiles of the density, temperature, stress and heat flux of the shock structures in argon for $Ma = 1.2, 2.0$ and 3.0 , respectively. For these cases, the distance x is normalised by the upstream mean free path $\lambda_1^{(2)}\sqrt{\pi}/2$. Our results are compared with the direct numerical solution of the full Boltzmann equation obtained by Ohwada (1993). We observe that the profiles of the density ($\delta\rho/\Delta\rho$) and temperature ($\delta T/\Delta T$) and the distance between these two profiles agree well with the numerical solutions of the Boltzmann equation (Ohwada, 1993). The normalised stress τ_{xx}/ρ_1RT_1 and heat flux $q_x/p_1(2RT_1)^{3/2}$ agree very well with the Boltzmann solution at $Ma = 1.2$ as shown in Figure 1, but show some increasing discrepancies at $Ma = 2.0$ and 3.0 . Because both the stress and heat flux sensitively depend on

the nonequilibrium part of the distribution function ($f - f^{(0)}$), which grows as the Mach number and/or the Knudsen number increase, it is understandable that the results from the modified GKS method, which only includes the second-order derivatives, deviate from the full Boltzmann solution.

It is known that various macroscopic or continuum methods (cf. Struchtrup, 2005), such as moment methods (Torrilhon and Struchtrup, 2004) and the Burnett equations (Uribe et al., 2000), have difficulties to deal with hypersonic shocks. Figure 4 presents the Mach-8 shock structures computed from the modified GKS method with $\nu = 12$, the DSMC results by Bird (1970) and experimental data by Schmidt (1969). Here, the distance x is normalised by the upstream mean free path $\lambda_1^{(1)}$, and the stress and heat flux are normalised as $\tau_{xx}/2\rho_1RT_1$ and $q_x/p_1(2RT_1)^{3/2}$, respectively. We also show the shock structures obtained by the GKS method with the collision time $\lambda = \mu/p$, which

Figure 4 Mach-8 shock structures in argon. The density and temperature profile (left), the normalised heat flux $q_x/\rho_1(2RT_1)^{3/2}$ (centre), and the normalised stress $\tau_{xx}/2\rho_1RT_1$ (right). Solid lines: modified-GKS results; dashed lines: Navier-Stokes results; Symbols: DSMC results (Bird, 1970); and dot-dashed line: experimental data (Schmidt, 1969)



is effectively a Navier-Stokes solver. From Figure 4, it is clear that the density and heat flux profiles obtained from the modified GKS method agree well with the DSMC results (Bird, 1970), and the density profile also agrees well with the experimental data (Schmidt, 1969). In the case of the stress, the modified GKS method correctly predicts the width, but over-predicts the peak value by about 40%. It is noted that the Navier-Stokes solver simply cannot correctly compute the shock structure—the shock is always too narrow, as clearly shown in Figure 4. It is also worth noting in Figure 4 that the values of the heat flux q_x computed from the modified GKS and DSMC methods is consistently larger than that obtained by the Navier-Stokes solver in the upstream part of the shock, consistent with previous observation (Elliot, 1975). Not only the heat flux profile obtained by the Navier-Stokes solver is much thinner, but also the location of the shock is shifted downstream. As for the stress τ_{xx} , both the modified GKS method and Navier-Stokes solver over-predict the peak value of τ_{xx} , and the overshoot in τ_{xx} seems to increase with the Mach number. The stress obtained by using the Navier-Stokes solver has a much narrower shock thickness than that obtained by the modified GKS method, which is rather close to the DSMC results in terms of the shock thickness. Overall, the results indicate that the modified GKS method with the limiter of Equation (29) can accurately predict shock structures in argon.

In Figure 5 we present the density profiles for Mach-9 and Mach-25 shocks in argon. The exponent ν is 7.5 and 9.0 for Mach-9 and Mach-25 shocks, respectively, in order to compare our results with experimental data (Alsmeyer, 1976) and the DSMC results (Bird, 1970). In the case of Mach-9 shock, the density profile obtained from the modified GKS method agrees very well with the experimental data (Alsmeyer, 1976), and in the case of Mach-25 shock, the modified-GKS results agree well with the DSMC ones (Bird, 1970). In both cases, the GKS Navier-Stokes results a narrower density profile across the shock, similar to the previous cases of lower Mach numbers.

Because the modified gas-kinetic scheme involves the derivatives of hydrodynamic variables and a nonlinear dynamic limiter, it would be interesting to investigate its behaviour when it is subject to grid refinement. To do so,

we compute the shock structures in argon at $Ma = 8.0$ by using about 35 ($N_x = 201$), 105 ($N_x = 601$) and 262 ($N_x = 1401$) grids inside the shock layer. The results for the density profile $(\rho(x) - \rho_1)/(\rho_2 - \rho_1)$ and the temperature profile $(T(x) - T_1)/(T_2 - T_1)$, the heat flux q_x and the stress τ_{xx} are showed in Figure 6(a)–(c), respectively. Clearly, the results obtained by using these three vastly different mesh sizes do not exhibit any visible difference, except the heat flux q_x . For the heat flux q_x , the peak value of q_x obtained with the coarsest mesh of 35 grid points within the shock differs only about 1% from that obtained with much finer meshes. Our results show that the modified gas-kinetic scheme is robust when subject to grid refinement.

The shock thickness is defined by

$$L_s = \frac{(\rho_2 - \rho_1)}{(d\rho/dx)_{\max}}.$$

Because the reciprocal density thickness λ_1/L_s can be measured experimentally (Alsmeyer, 1976) and therefore it is useful for validating numerical results (Reese et al., 1995). We use two values of the exponent ν , 7.5 and 9.0, to compute the reciprocal density thickness λ_1/L_s , where λ_1 is given by Equation (37). In Figure 7, the reciprocal density thickness λ_1/L_s computed by using the modified GKS method are compared with the experimental data collected by Alsmeyer (1976). Obviously, the shock thickness depends on the molecular interaction characterised by the exponent ν , which is used as adjustable parameter here. Clearly, for hypersonic shocks, the modified GKS method can yield the reciprocal density thickness λ_1/L_s in better agreement with the experimental data than the Navier-Stokes results. In general, the shock computed from the Navier-Stokes equations is thinner. The effect of the exponent ν is also clearly shown in Figure 7: The larger ν or the harder the potential is, the thinner the shock is. We should also point out that the modified-GKS method does not dramatically improve the results of the reciprocal shock thickness λ_1/L_s when compared that obtained by the Navier-Stokes equations, especially when the exponent ν can be used as an adjustable parameter. However, when we look at the results of the heat flux q_x and the stress τ_{xx} of Figure 4, the improvement is indeed considerable. This indicates that, while the shock thickness is a necessary

Figure 5 Mach-9 (left) and Mach-25 (right) shock density profiles in argon. The x is normalised by $\lambda_1^{(2)}$ and $\lambda_1^{(1)}$ for Mach-9 and Mach-25 shock, respectively. Solid lines: modified-GKS results; dashed lines: Navier-Stokes results; bullets: experimental data (Alsmeyer, 1976); and squares: DSMC results (Bird, 1970)

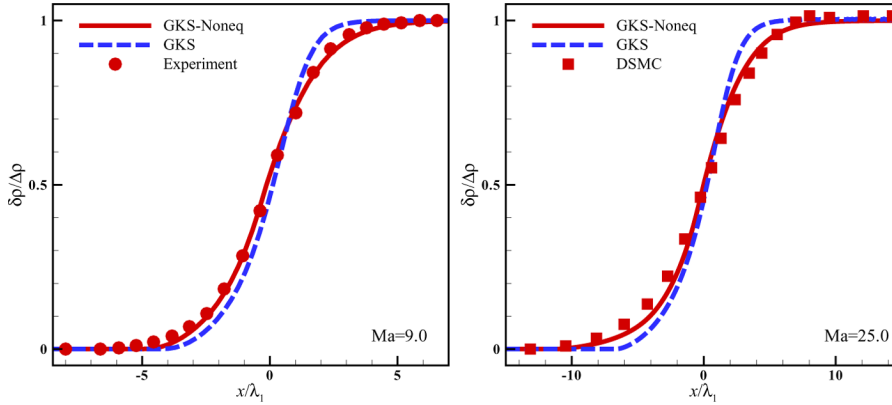
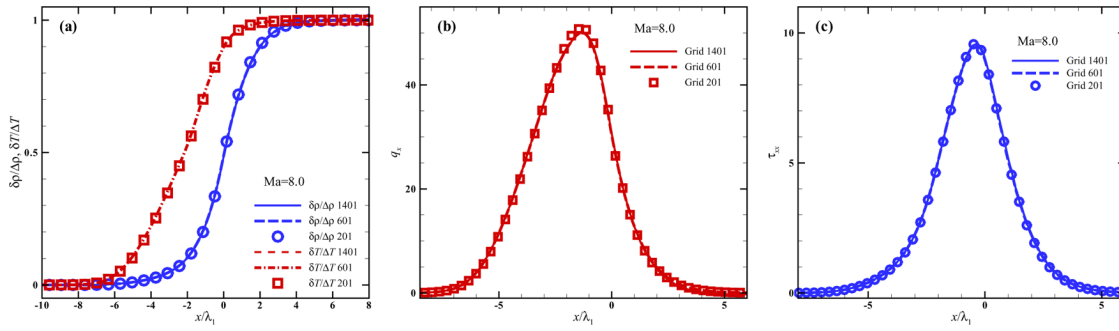


Figure 6 Grid dependence of the shock structures inside the shock layer in argon at $Ma = 8.0$. (a) the density $(\rho(x) - \rho_2)/(\rho_1 - \rho_2)$ and temperature $(T(x) - T_2)/(T_1 - T_2)$ profiles; (b) the heat flux q_x , and (c) the stress τ_{xx}



and good measure of shock structure, it is nonetheless an insufficient one to test numerical methods for shock structures.

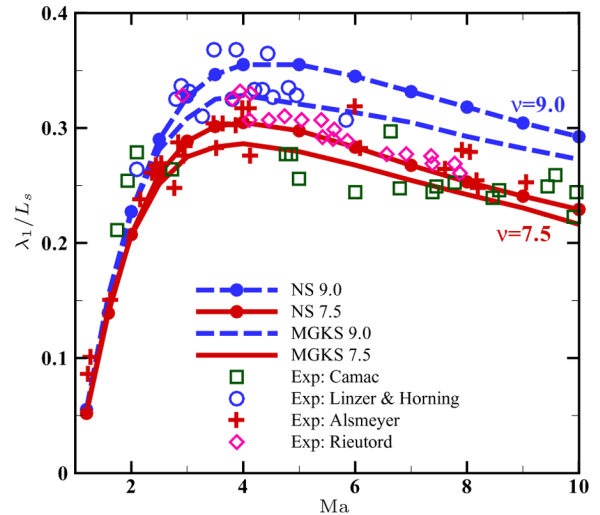
4 Conclusion

We present in this paper a modified gas-kinetic scheme with a variable local collision time λ^* depending on the gradients of the hydrodynamic variables up to second order. We use the modified gas-kinetic scheme to compute stationary shock structures in argon with the Mach number Ma between 1.2 to 25.0. Our results are validated with numerical solutions of the full Boltzmann equation for $Ma = 1.2, 2.0$ and 3.0 and with the DSMC results for $Ma = 8.0$ and 25.0 . We also verified our results with available experimental data for $Ma = 8.0$ and 9.0 . We computed profiles of the density, the temperature, the heat flux, and the stress across the shock. The Mach number dependence of the reciprocal shock thickness λ_1/L_s is also computed and compared with experimental data for Ma between 1.2 and 10.0.

Our results generally agree well with those obtained by the DSMC method, the full Boltzmann equation, and available experimental data, in terms of the density and temperature profiles, the heat flux, and the stress across the shock. The greatest discrepancy is in the calculations of the

stress τ_{xx} : The modified GKS over-predicts the peak value of τ_{xx} , although the width of τ_{xx} is correctly predicted, when compared with DSMC results.

Figure 7 The Mach number dependence of the reciprocal shock thickness λ_1/L_s in argon. Lines without symbols: modified-GKS results. Lines with solid circles: Navier-Stokes results. Solid lines $\nu = 7.5$ and dashed lines $\nu = 9.0$. Symbols: experimental data. \circ : Linzer & Horning; \square : Camac; $+$: Alsmeyer; and \diamond : Rieutord (cf. Alsmeyer, 1976)



The modified GKS method is a simple extension of the GKS method for the compressible Navier-Stokes equations. It is essentially a continuum approach. Our results show that the modified GKS method is an effective and efficient method for shock structure calculations. For a typical mesh of $N_x \times N_y = 201 \times 3$ used in our calculations, the CPU time on an AMD 2.2GHz Opteron processor is over one minute for 30,000 iterations to obtain a converged stationary shock. This is orders of magnitude faster than the DSMC method or the CFD-DSMC hybrid scheme (Schwartzentruber and Boyd, 2006; Schwartzentruber et al., 2007).

We should also point out the limitations of the modified GKS method for near-continuum flows. First of all, the modified GKS method is based on the BGK model, which is a special case of the linearised Boltzmann equation. Therefore it inherits all the deficiencies and limitations of the BGK model: it has only one parameter λ which determines all the transport coefficients (Struchtrup, 2005), for example. Secondly and more importantly, the modified GKS method is an extension of the Navier-Stokes equations. It is not a solution method for the distribution function f . Therefore, it is limited to the flows not far from equilibrium. To overcome these limitations, more sophisticated collision models must be considered. And finally, the limiter of Equation (29) used in the modified GKS method is a heuristic approach which deserves further investigation. Although the modified GKS method has been shown to be effective for computing shock structures, it is not yet clear if it can be effective for more complex non-equilibrium flows. This will be the subject of our future investigation.

Acknowledgements

W. Liao, Y. Peng and L-S. Luo would like to acknowledge the support from the US Department of Defense under AFOSR-MURI project "Hypersonic Transition and Turbulence with Non-equilibrium Thermochemistry" (Dr. J. Schmisser, Program Manager) and from NASA Langley Research Center C&I Program through National Institute of Aerospace under the Cooperative Agreement Grant NCC-1-02043. K. Xu would like to acknowledge the support from Research Grants Council of the Hong Kong Special Administrative Region, China, under the Projects 6210/05E and 6214/06E.

References

- Alsmeyer, H. (1976) 'Density profiles in argon and nitrogen shock waves measured by the absorption of an electron beam', *J. Fluid Mech.*, Vol. 74, April, pp.497–513.
- Bergemann, F. and Brenner, G. (1994) 'Investigation of wall effects in near continuum hypersonic flow using the DSMC method', AIAA Paper 1994-2020.
- Bhatnagar, P., Gross, E. and Krook, M. (1954) 'A model for collision processes in gases', *Phys. Rev.*, Vol. 94, pp.511–525.
- Bird, G.A. (1970) 'Aspects of the structure of strong shock waves', *Phys. Fluids*, Vol. 13, No. 5, pp.1172–1177.
- Bird, G.A. (1994) *Molecular Gas Dynamics and the Direct Simulations of Gas Flows*, Oxford Science, Oxford, UK.
- Boyd, I. and Gokcen, T. (1992) 'Evaluation of thermochemical models for particle and continuum simulations of hypersonic flow', AIAA Paper 1992-2954.
- Cercignani, C. (1988) *The Boltzmann Equation and Its Applications*, Springer, New York.
- Chapman, S. and Cowling, T.G. (1952) *The Mathematical Theory of Nonuniform Gases*, Cambridge University Press, Cambridge, UK.
- Elizarova, T.G., Shirokov, I.A. and Montero, S. (2005) 'Numerical simulation of shock-wave structure for argon and helium', *Phys. Fluids*, Vol. 17, No. 6, p.068101.
- Elliot, J.P. (1975) 'On the validity of the Navier-Stokes relation in a shock wave', *Can. J. Phys.*, Vol. 53, No. 6, pp.583–586.
- Harris, S. (2004) *An Introduction to the Theory of Boltzmann Equation*, Holt, Rinehart and Winston, New York, 1971, Reprinted by Dover.
- Holden, M. (2000) 'Experimental studies of laminar separated flows induced by shock wave/boundary layer and shock/shock interaction in hypersonic flows for CFD validation', AIAA Paper 2000-0930.
- Ivanov, M.S. and Gimelshein, S.F. (1998) 'Computational hypersonic rarefied flows', *Annu. Rev. Fluid Mech.*, Vol. 30, pp.469–505.
- Ohwada, T. (1993) 'Structure of normal shock waves: direct numerical analysis of the Boltzmann equation for hard-sphere molecules', *Phys. Fluids*, Vol. 5, No. 1, pp.217–234.
- Ohwada, T. and Xu, K. (2004) 'The kinetic scheme for the full-Burnett equations', *J. Comput. Phys.*, Vol. 201, No. 1, pp.315–332.
- Reese, J.M., Wood, L.C., Thivet, F.J.P. and Candel, S.M. (1995) 'A second-order description of shock structure', *J. Comput. Phys.*, Vol. 117, p.240.
- Rosenau, P. (1989) 'Extending hydrodynamics via the regularization of the Chapman-Enskog expansion', *Phys. Rev. A*, Vol. 40, No. 12, pp.7193–7196.
- Schmidt, B. (1969). 'Electron beam density measurements in shock waves in argon', *J. Fluid Mech.*, Vol. 39, pp.361–373.
- Schwartzentruber, T.E. and Boyd, I.D. (2006) 'A hybrid particle-continuum method applied to shock waves', *J. Comput. Phys.*, Vol. 215, No. 2, pp.402–416.
- Schwartzentruber, T.E., Scalabrin, L.C. and Boyd, I.D. (2007) 'A modular particle-continuum numerical method for hypersonic non-equilibrium gas flows', *J. Comput. Phys.*, Vol. 225, No. 1, pp.1159–1174.
- Struchtrup, H. (2005) *Macroscopic Transport Equations for Rarefied Gas Flows*, Springer, Berlin.
- Torrilhon, M. and Struchtrup, H. (2004) 'Regularized 13-moment equations: Shock structure calculations and comparison to Burnett models', *J. Fluid Mech.*, Vol. 13, pp.171–198.
- Uribe, F.J., Velasco, R.M., Garcia-Colin, L.S. and Diaz-Herrera, E. (2000) 'Shock wave profiles in the Burnett approximation', *Phys. Rev. E*, Vol. 62, p.6648.

- van Leer, B. (1974) 'Towards the ultimate conservative difference scheme II. Monotonicity and conservation combined in a second order scheme', *J. Comput. Phys.*, Vol. 14, No. 4, pp.361–370.
- Woods, L.C. (1993) *An Introduction to the Kinetic Theory of Gases and Magnetoplasmas*, Oxford University Press, Oxford, UK.
- Wu, J-S. and Tseng, K-C. (2003) 'Parallel particle simulation of the near-continuum hypersonic flows over compression ramps', *J. Fluids Eng.*, Vol. 125, No. 1, pp.181–188.
- Xu, K. (1998) 'Gas-kinetic schemes for unsteady compressible flow simulations', *29th Computational Fluid Dynamics*, VKI Lecture Series, Vol. 1998-03, The von Karman Institute for Fluid Dynamics, Rhode-St-Genèse, Belgium, pp.1–202.
- Xu, K. (2001) 'A gas-kinetic BGK scheme for the Navier-Stokes equations and its connection with artificial dissipation and Godunov method', *J. Comput. Phys.*, Vol. 171, No. 1, pp.289–335.
- Xu, K. and Josyula, E. (2006) 'Continuum formulation for non-equilibrium shock structure calculation', *Comm. Comput. Phys.*, Vol. 1, No. 3, pp.425–450.
- Xu, K. and Tang, L. (2004) 'Nonequilibrium Bhatnagar-Gross-Krook model for nitrogen shock structure', *Phys. Fluids*, Vol. 16, No. 10, pp.3824–3827.
- Zheng, Y.S., Reese, J.M. and Struchtrup, H. (2006) 'Comparing macroscopic continuum models for rarefied gas dynamics: a new test method', *J. Comput. Phys.*, Vol. 218, No. 2, pp.748–769.